Photochemistry and Photobiology, 2007, 83: 958–965

Polymeric Photosensitizer Prodrugs for Photodynamic Therapy

Marino A. Campo[1], Doris Gabriel[1], Pavel Kucera[2], Robert Gurny[1] and Norbert Lange*[1]

[1]Laboratory of Pharmaceutics and Biopharmaceutics, Section of Pharmaceutical Sciences, Université Lausanne, Université Geneva, Geneva, Switzerland
[2]Institut de Physiologie, Faculté de Médicine, Université de Lausanne, Lausanne, Switzerland

Received 12 September 2006; accepted 13 February 2007, DOI: 10.1111/j.1751-1097.2007.00090.x

ABSTRACT

A targeting strategy based on the selective enzyme-mediated activation of polymeric photosensitizer prodrugs (PPP) within pathological tissue has led to the development of agents with the dual ability to detect and treat cancer. Herein, a detailed study of a simple model system for these prodrugs is described. We prepared "first-generation" PPP by directly tethering the photosensitizer (PS) pheophorbide a to poly-(L)-lysine *via* epsilon amide links and observed that by increasing the number of PS on a polymer chain, energy transfer between PS units improved leading to better quenching efficiency. Fragmentation of the PPP backbone by trypsin digestion gave rise to a pronounced fluorescence increase and to more efficient generation of reactive oxygen species upon light irradiation. *In vitro* tests using the T-24 bladder carcinoma cell line and *ex vivo* experiments using mouse intestines illustrated the remarkable and selective ability of these PPP to fluoresce and induce phototoxicity upon enzymatic activation. This work elucidated the basic physicochemical parameters, such as water solubility and quenching/activation behavior, required for the future elaboration of more adaptable "second-generation" PPP, in which the PS is tethered to a proteolytically stable polymer backbone *via* enzyme-specific peptide linkers. This polymer architecture offers great flexibility to tailor make the PPP to target any pathological tissue known to over-express a specific enzyme.

INTRODUCTION

Since its introduction by von Tappeiner and Jesionek (1) and Raab (2) at the beginning of the 20th century, photodynamic therapy (PDT) has evolved into a powerful modality for the treatment of a wide range of pathological conditions (3,4), among which are certain types of cancer, precancerous conditions, age-related macular degeneration (5), as well as anti-parasitic and antibacterial applications (6–8). Briefly, PDT is based on the administration of a photosensitizer (PS), which upon external irradiation with nonionizing light becomes excited and transforms molecular oxygen present in the tissue into reactive oxygen species (ROS), such as singlet oxygen. Subsequently, the targeted tissue is destroyed after a complex cascade of chemical, biological and physiological reactions (3). In spite of its promises, this treatment modality is still somewhat limited by an unfavorable PS biodistribution and insufficient selectivity toward pathological tissue, giving rise to serious unwanted side effects, such as long-lasting skin photosensitization (9,10). While the latter has been resolved by the introduction of second-generation PS the former has been shown to be more difficult to address until today.

Besides improving their water solubility, tethering PS to a designed polymer carrier has two main advantages in terms of tissue targeting selectivity, namely, higher molecular weight entities will accumulate passively in tumors due to the enhanced permeability and retention effect (EPR) (11), and the specific activation/release of the PS through tumor-associated enzymes, such as matrix metalloproteinases (MMPs), cathepsins, plasmin, *etc*. (12–14), will be quite specific.

Our targeting strategy is based on the use of protease-sensitive polymeric photosensitizer prodrugs (PPP), which are expected to display diminished photoactivity in their native state due to efficient energy transfer between closely spaced PS units (15). However, enzymatic fragmentation of the PPP would have a photo-activating effect due to an increase in PS's mutual distance. Degradation of the poly-L-lysine backbone of first-generation conjugates (Type A cleavage, Fig. 1) is expected to occur mainly through cleavage by lysosomal cysteine- and serine-proteases (*e.g*. cathepsin B and trypsin-like serine proteases). Up-regulation of these enzymes has been demonstrated in many human tumors, including breast, lung, brain, gastrointestinal, head and neck cancers.

However, in order to effectively target a particular enzyme, which varies on the type of cancer and even stage of the disease, the polymeric carrier must be easily adapted to be activated by the enzyme of interest. Besides cysteine and serine proteases (*e.g*. plasmin, uPA, tPA, kallikreins), aspartyl proteases (cathepsin D) and MMPs are considered major contributors of the overall pro-proteolytic imbalance characterizing tumor growth or inflammatory processes. This could be accomplished by the use of specific cleavable peptidic linkers tethering the PS to the polymer backbone (see Fig. 1). Thus, the appropriate amino acid sequence in the linker will dictate which enzyme is being targeted (16–22).

Before developing these highly sophisticated "second-generation" PPP, it is of the essence to first understand the parameters dictating PPP quenching/activation and solubility using a simpler model system, which we have defined as "first-generation" PPP. Similar "first-generation" conjugates made by tethering chlorine e6 directly to PLL-PEG [PPL; poly(L-lysine)] have been recently reported by Choi *et al*.

*Corresponding author email: norbert.lange@pharm.unige.ch (Norbert Lange)

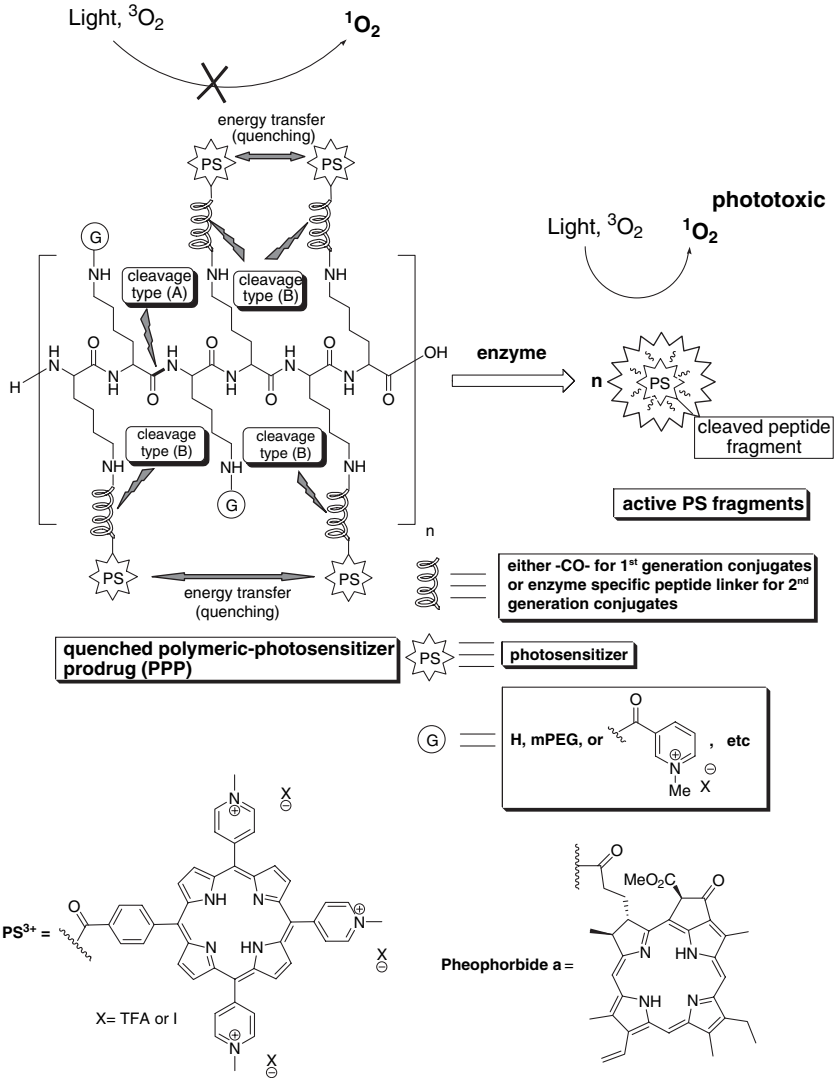

Figure 1. Schematic representation of PPP architectures and mechanisms involved in enzyme-mediated photosensitization. Polymeric constructs carrying photosensitizer (PS) moieties only generate ROS upon enzymatic digestion and subsequent irradiation with light. Here, activation is accomplished by the enzyme through either type (A) cleavage (G = H) of the PLL backbone in the case of first-generation conjugates (enzymes targeted: trypsin and cathepsins) or by type (B) cleavage.

(20,21). These first-generation PPP can be assembled by directly tethering the PS to a PLL *via* epsilon amide functions (see Fig. 1), thus providing a simple model to study the basic physicochemical parameters and quenching/activation phenomena of such macromolecular entities. The main difference between these two architectures is that activation of first-generation PPP involves backbone degradation (type A cleavage, Fig. 1), while that of the second generation involves site-specific cleavage of the peptidic linkers (type B cleavage, Fig. 1).

In the present study, we investigated the fundamental properties of such first-generation PPP with respect to their fluorescence quenching, photodynamic activity and water solubility. Furthermore, we have explored novel strategies that will (1) improve the water solubility of the PPP, (2) significantly improve the quenching/activation characteristics, (3) provide easy means to totally protect the backbone against nonspecific enzymatic degradation and (4) allow for simple modulation of pharmacokinetics.

MATERIALS AND METHODS

Reagents. All commercial reagents were used as obtained. Anhydrous forms of *N*,*N*-dimethylformamide (DMF), dimethylsulfoxide (DMSO), dichloromethane (DCM), diethyl ether, and ethyl acetate, as well as *N*-(3-dimethylaminopropyl)-*N*'-ethyl-carbodiimide hydrochloride (EDC), *N*-hydroxysuccinimide, *N*,*N*-diisopropylethylamine (DIPEA), porcine trypsin, PLL HBr (25 KDa, DP = 118.5, PD = 1.4; and 7.4 KDa, DP = 35.5, PD = 1.6), dimethyl glycine, methyl iodide, pyrrole, 4-carboxybenzaldehyde, 4-pyridinecarboxaldehyde and nicotinic acid were purchased from Fluka (Buchs, Switzerland). Pheophorbide a was purchased from Frontier Scientific (Logan, UT). D-PBS solution was purchased from GIBCO (Invitrogen, Basel, Switzerland). mPEG-NHS ester (5 KDa) was purchased from Nektar Therapeutics (Huntsville, AL).

General procedures. All ^1H and ^{13}C spectra were recorded at 300 and 75.5 Hz, respectively, using a Bruker NMR spectrometer (Bruker, Karlsruhe, Germany). Mass spectra were recorded using a Finnigan MAT SSQ 7000 (Thermo Electron Co., Waltham, MA). Fluorescence photodetection (FPD) was performed with a Karl-Storz D-light system fitted to a cystoscope (Karl Storz, Tuttlingen, Germany).

Pheophorbide a-NHS ester (22). To a solution of pheophorbide a (300 mg, 0.506 mmol) in CH_2Cl_2 (95 mL) were added EDC (1.7 equiv, 0.165 g), *N*-hydroxysuccinimide (1.7 equiv, 0.10 g) and DMAP (0.4 equiv, 24 mg) and the mixture stirred for 16 h under argon in the dark. Solvent was removed under reduced pressure and the product purified by flash chromatography on a silica gel column using CH_2Cl_2/EtOAc 40:60. The product was obtained as a dark solid (230 mg, 66% yield) and characterized by ^1H and ^{13}C NMR spectroscopy. ESI-MS: 712.7 ($[M + Na]^+$, $C_{39}H_{39}N_5O_7Na^+$). ^1H NMR (300 MHz, DMSO): 9.54(s, 1H), 9.07(s, 1H), 8.83(s, 1H), 7.95(dd, J = 18,12 Hz, 1H), 6.43(s, 1H), 6.23(d, J = 19 Hz, 1H), 6.01(d, J = 12 Hz, 1H), 4.62–4.66(m, 1H), 4.12(br. d, J = 10 Hz, 1H), 3.84(s, 3H), 3.56(s, 3H), 3.05–2.95(m, 1H), 2.94–2.64(m, 15H), 1.78(d, J = 7 Hz, 3H), 1.48(t, J = 7 Hz, 3H), 0.19(s, 1H), −2.06(s, 1H) p.p.m. ^{13}C NMR (75.5 Hz, DMSO): 10.5, 11.6, 11.8, 17.2, 18.3, 22.7, 25.4, 27.7, 28.6, 48.9, 50.4, 52.7, 64.2, 93.8, 96.7, 104.5, 105.4, 123.0, 128.2, 128.5, 128.7, 132.1, 135.3, 135.6, 136.0, 137.7, 141.3, 144.8, 148.7, 150.1, 154.6, 161.0, 168.7, 169.2, 170.2, 172.8, 189.1 p.p.m. (missing one sp^2 carbon).

5-(4-(N-oxycarbonylsuccinimide)phenyl)-10,15,20-tris(4-(N-methyl pyridyl) porphyrin tetraiodide. This compound was prepared in three steps according to a literature procedure by Tomé *et al*. The spectral properties were identical to those previously reported (23).

N-Succinimidyl (1-methyl-3-pyridinio)formate iodide. This compound was prepared in two steps from nicotinic acid according to a literature procedure (24). The spectral properties were identical to those previously reported (24).

Ethanaminium 2-[(2,5-dioxo-1-pyrrolidinyl)oxy]N,N,N-trimethyl-2-oxo iodide. This compound was prepared from *N,N*-dimethylglycine by a similar procedure described previously (24,25).

General procedure for the preparation of pheophorbide-poly(L-lysine) conjugates. To a solution of PLL HBr (25 KDa, DP = 118.5) (8.0 mg, 3.83×10^{-5} mol of epsilon NH_2 functions) in anhydrous DMSO (0.84 mL) was added DIPEA (3.0 equiv per epsilon NH_2, 14.9 mg). Thereafter, the corresponding amount of pheophorbide a-NHS ester in DMSO (7 mg mL^{-1}) was added under vigorous stirring to obtain PPP loaded with an average of 1 (0.22 mg of PS-NHS), 6 (1.34 mg of PS-NHS), 12 (2.68 mg of PS-NHS), 18 (4.01 mg of PS-NHS), 24 (5.35 mg of PS-NHS) and 30 (6.69 mg of PS-NHS) PS units per PLL (25 KDa) chain. The progress of this quantitative coupling reaction was monitored by analytical HPLC (LaChroma; Merck, Darmstadt, Germany) using a C18 column (Macharey Nagel, Basel, Switzerland) and water/acetonitrile/TFA (50:50:0.001) as eluent. Thus, the gradual disappearance of the reference peak corresponding to pheophorbide a-NHS and the appearance of a broad and more polar peak corresponding to the PPP was monitored by UV/VIS ($[\lambda_{abs}$ = 405 nm)] and fluorescence detection [λ_{ex} = 405 nm, λ_{em} = 670 nm]) using this system. The reaction mixture was then quenched by adding water (3.0 mL) and TFA to pH 2–3. The resulting solution was filtered and purified by size exclusion chromatography using a sephacryl™ S-100 (Amersham Biosciences, Otelfingen, Switzerland) column and 30:70:0.00025 acetonitrile/water/TFA as eluent. The fraction containing the product was lyophilized to yield the desired product as a green solid. UV/VIS (H_2O): 287.6 (29 707 M^{-1} cm^{-1}), 390.0 (1 22 128 M^{-1} cm^{-1}), 504.4 (13 803 M^{-1} cm^{-1}), 623.6 (8402 M^{-1} cm^{-1}), 667.6 (43 510 M^{-1} cm^{-1}).

The pheophorbide a-PLL conjugate made with 7.4 KDa (DP = 35.5) PLL was prepared in the same manner as the conjugates made with 25 KDa PLL.

For the preparation of conjugates carrying moieties besides the PS, the proper amount of NHS-activated reagent in DMSO was added drop wise to the reaction mixture containing the PS–PLL conjugate and the reaction allowed to proceed for an additional 3 h prior to the workup and purification steps.

The 5-(4-carboxyphenyl)-10,15,20-tris(4-(N-methylpyridyl) porphyrin-PLL (PS^{3+}-PLL) conjugate was prepared according to the procedure of Tomé *et al*. (23).

The reproducibility of conjugate preparation was performed by preparing triplicates of each conjugate and then comparing their photophysical properties. It was observed that within the same batches of PLL, there was less than 5% average deviation on the quenching factor but larger deviations were observed when using different batches of commercially available PLL (up to 10%).

Fluorescence measurements. A volume of 0.02 mL of the stock solution containing the corresponding conjugate in DMSO (1.0–0.1 m*M*) with respect to pheophorbide a) was diluted in 1.0 mL of D-PBS buffer. From this solution, two 0.5 mL aliquots were taken and incubated separately at 37°C after adding either 0.05 mL of D-PBS solution to the control or 0.05 mL of trypsin-EDTA solution (0.5 g of porcine trypsin, 0.2 g of EDTA, and 4.0 g Na/L HBSS) (Sigma, Buchs, Switzerland). Fluorescence intensity was followed overtime at 37°C using a SPEX Fluoromax (Perkin-Elmer, Wellesley, MA) excitation at 400 nm and emission at 670 nm.

In vitro cell experiments. The green fluorescent protein-transfected T-24 bladder carcinoma cell line was kindly provided by S. Clouthier from the Lausanne's CHUV Hospital (Switzerland) and grown to confluence in 96 well plates using DMEM medium supplemented with 10% heat-inactivated fetal calf serum and 1% penicillin/streptomycin (10 000 U mL^{-1}:10 000 μg mL^{-1}) (complete medium) under a humidified 5% CO_2 atmosphere. Cells were incubated with the PPP loaded with 18 pheophorbide a moieties per chain in D-PBS buffer/complete medium (1:3) at different concentrations for 30 min and washed three times with fresh HBSS buffer before PDT with white light (27 J cm^{-2}). Cell viability was determined by the (3–(4,5-dimethyl)thiazol-yl)-2, 5-diphenyl tetrazolium bromide (MTT) test 24 h after irradiation. The "dark" toxicity of the PPP was obtained by using a controlled experiment in which cells were not irradiated. Activation of the PPP was accomplished by digesting the compound with trypsin (0.167 mg mL^{-1}) for 15 min at 37°C followed by enzyme inactivation with 4-aminobenzamidine (1.1 mg mL^{-1}). In order to maintain homologous experimental conditions, the solutions of the inactivated control PS-PL conjugates also contained trypsin + 4-aminobenzamidine (inactivated trypsin = (−)).

Ex vivo tissue experiments. Freshly excised jejunum (upper 10 cm of small intestine) and colon (lower 3.0 cm segment) from two mice (C57BL6/J) were placed on a well oxygenated Hartmann solution. The organs were perfused with 1.0 mL of the saline solution and then instilled with an oxygenated 0.9% saline solution containing a PPP loaded with 18 PS units per chain at a concentration corresponding to 5.0 μ*M* of the PS and trypsinogen (50 μg mL^{-1}). As a control, a jejunum was also instilled with an oxygenated 0.9% saline containing the PPP but without trypsinogen. The intestinal segments were incubated at 37°C under a humidified 5% CO_2 atmosphere for 1 h. Previous to FPD, the instilled solutions were evacuated from the intestinal segments and replaced by 0.9% saline. The tissues were photographed under white and blue light illumination with the Storz-D light system.

ROS measurements in aqueous media using iodide. This is a modified procedure previously described by Mosinger and Micka (26), in which we monitored the I_3^- (286 nm absorbance band) generated by ROS oxidation of I^- in aqueous media. We prepared aqueous D-PBS buffered solutions of all the PPP setting the pheophorbide a concentration to 3.5 μ*M* by adjusting the optical density at 667 nm to 0.125. Each of the equimolar solutions was treated in the following fashion. To 0.6 mL of a given PPP in buffered solution was added 0.2 mL of 2.50 *M* NaI (aq) and the UV-vis spectra was recorded as background. Then, this solution was placed in the well of a cell culture plate (24 wells), where it was irradiated with white light for 2 min (3.72 J cm^{-2}). The UV-Vis spectrum was again recorded and the background absorbance at 286 nm subtracted to yield the actual increase in optical density; then, the following formula was used to calculate the normalized increase in optical density at 286 nm (value = [actual increase in optical density for PPPx − actual increase in optical density for reference PPP (loaded with 1 PS unit per chain)]/actual increase in optical density for reference PPP).

RESULTS AND DISCUSSION

We started assembling model PS-polymer conjugates by coupling the PS pheophorbide a-NHS ester to PLL in view of the components' commercial availability, ease of modification, and the chemical stability and biodegradability of the polymer, as well as its documented medical use (27–29). The coupling of varying amounts of pheophorbide a-NHS ester

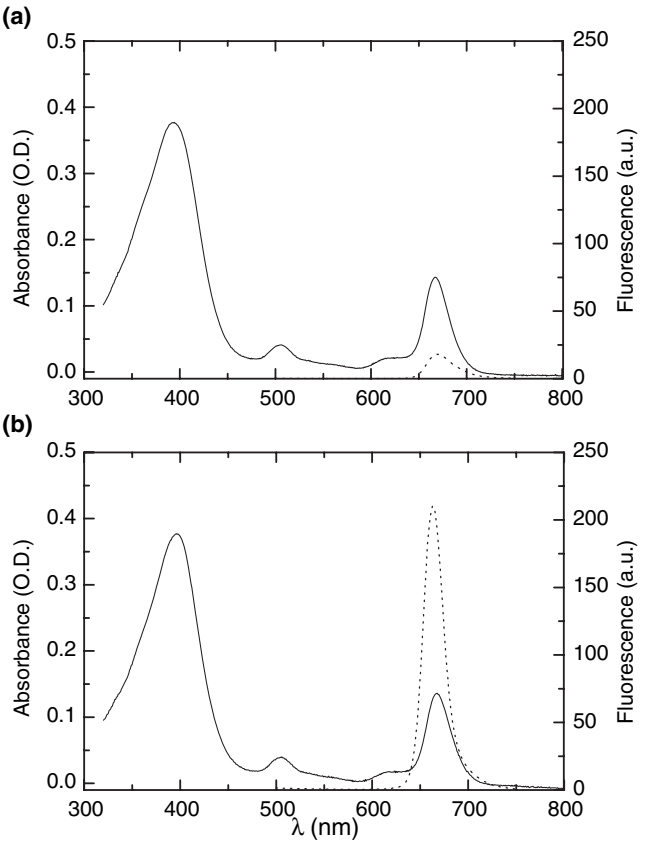

Figure 2. Typical adsorption (solid lines) and emission spectra (dotted lines) in aqueous PBS buffer of a first-generation PPP loaded with 18 pheophorbide a moieties per polymer chain in its native (a) and activated (b) forms.

(22) to PLL·HBr (25 KDa, DP = 118.5) was monitored over time using HPLC analysis. The reaction was shown to be quantitative by following the complete disappearance of the peak corresponding to pheophorbide a-NHS (λ_{abs} = 400 nm) and the appearance of a new, more polar, broad peak corresponding to the PPP, thus providing conjugates with an estimated average of 1, 6, 12, 18, 24 and 30 PS units per polymer chain. Figure 2 shows the corresponding absorption (solid lines) and emission (dotted lines) spectra of a PPP loaded with 18 PS units per polymer chain in its native (Fig. 2a) and activated (Fig. 2b) forms. The fluorescence quenching factor increased as a function of number of PS units in a polymer chain, revealing that at equimolar concentrations of the PS (equiabsorbant solutions at 667 nm), better fluorescence quenching is observed for higher PS loading (Table 1). This is consistent with the idea that higher PS loadings on a polymer chain lead to shorter average distances between PS and thus to better energy transfer (22), which is in turn proportional to $1/R^6$ (R is the mutual PS distance) (15). A rough estimate of the maximum theoretical distance between PS in these PPP was estimated to be > >450, 90, 41, 26, 20 and 16 Å for the PPP carrying 1, 6, 12, 18, 24 and 30 PS respectively (assuming PLL is a stretched-out chain with 3.8 Å per amino acid residue [30]). It was somewhat surprising to find that, based on the known 62 Å Förster radius for pheophorbide a (31), the expected number of PS residues per chain required to have a quenching efficiency of 50% was approximately 9. The data, however, show that with only six pheophorbide a residues per chain, the quenching efficiency is already 97% (calculated R = 35 Å), indicating that the PPP must adopt a conformation other than a stretched-out random coil (32,33), which allows for the PS units to be in close proximity to one another.

Fluorescence quenching becomes highly efficient for PPP loaded with 18 PS units or more (fluorescence quenching factor ≥ 131.7 or quenching efficiency ≥ 99.2%; see Table 1). Unfortunately, due to limited water solubility, conjugates with higher than 30 PS per chain could not be tested (see Table 1).

Enzymatic trypsin digestion of the PLL backbone was used to activate the PPP in aqueous media (PBS buffer) and the fluorescence intensity of the PPP + trypsin mixture monitored over time. All of the PPP showed a similar Michaelis–Menten kinetics behavior, which consisted of the characteristically fast initial fluorescence increase which gradually decreased and the fluorescence value reached a plateau after a certain time

Table 1. Effect of covalently linking increasing amounts of pheophorbide a to PLL·HBr (25 KDa) on the quenching/activation behavior and on the conjugate water solubility.

PS units/ PLL chain	Water solubility (in terms of PS concentration [mM])	Quenching efficiency* (1-FL /F_o)	Quenching factor* (F_o /FL)	Fluorescence increase upon enzymatic activation†	Relative photodynamic response‡ (optical density at 286 nm)
1	>10	0	1	1.1 ± 0.2	1.0 ± 0.05
6	>10	0.972	35.4	6.0 ± 0.5	0.25 ± 0.02
12	8.2	0.978	46.0	18.8 ± 1.2	0.070 ± 0.002
18	1.3	0.992	131.7	12.0 ± 0.5	0.050 ± 0.001
24	0.2	0.993	145.8	8.1 ± 0.5	0.035 ± 0.001
30	0.01	0.998	626.8	5.9 ± 0.4	0.024 ± 0.002

F_o = fluorescence intensity of the nonquenched conjugate carrying one PS unit per chain; FL = fluorescence intensity of conjugate carrying a given number of PS unit per chain. *Measurements were carried out under identical concentrations of the PS by adjusting the optical density at 667 nm. †Maximum PPP fluorescence activation value (FL_{max}/FL, where FL is fluorescence value of the corresponding undigested PPP, and FL_{max} is maximum fluorescence value attained upon activation) upon digestion with trypsin. ‡Relative photodynamic response of PPP was noted by irradiating with white light (3.72 J cm^{-2}) the solutions containing the PPP + NaI under equimolar concentration of the PS. Photodynamic response of the unactivated was measured by monitoring the increase in optical density at 286 nm corresponding to the absorption band of the triiodide (I_3^-) generated by ROS-mediated oxidation of NaI. The following formula was used to calculate the normalized increase in optical density at 286 nm (value = [actual increase in optical density for PPPx − actual increase in optical density for reference PPP (loaded with 1 PS unit per chain)]/actual increase in optical density for reference PPP).

period. On the other hand, the PPP were chemically stable under physiological pH (PBS buffer) in the absence of the enzyme, and their fluorescence intensity remained constant over time. The activation phenomenon was quantified for each of the PPP and expressed as the ratio of the conjugate's maximum fluorescence value (FL_{max}), obtained after trypsin activation, and baseline fluorescence (FL_o), corresponding to the nonactivated PPP. Thus, the activation of PPP carrying 1, 6, 12, 18, 24 and 30 PS moieties per chain gave fluorescence increases of 1, 6, 19, 12, 8 and 6 times, respectively (see Table 1). Notice that the PPP carrying 12 PS per chain gave the highest activation increase, corresponding to a value of 19. This may indicate that the mutually exclusive effects of quenching and enzymatic digestion are optimal for the activation of this particular PPP. Although higher PS loading leads to increasingly better quenching of the PPP in its native state, enzymatic digestion becomes progressively more difficult as the key lysine side chains of PLL required for enzyme recognition and cleavage have been extensively modified. This situation leads to poor fluorescence activation of a very well quenched PPP due to the lack of enzymatic digestion. On the contrary, low PS loading leads to less efficient quenching but superior enzymatic digestion of the polymeric backbone, which results in poor fluorescence activation because the PPP was already fluorescent in its native state.

Efficient quenching of the PS singlet state leads to fluorescence decrease upon excitation with light; similarly, the triplet state in these PPP should also be inactivated by mutual energy transfer, which would result in a diminished ability to generate ROS and thus in reduced PPP phototoxicity. This triplet inactivation was determined indirectly by measuring the amount of ROS generated by the PPP under identical irradiation conditions and concentration of the PS (photodynamic response) by using an iodide assay described by Mosinger and Micka (26). The photodynamic activity of the conjugates decreased with increasing number of PS units on the polymer chain (Table 1). Therefore, similar to the fluorescence quenching, triplet state inactivation also improved by increasing the number of PS on a chain. Thus, we can conclude that proper PS loading would lead to PPP that are nonfluorescent and nonphototoxic.

In this context one should consider that pheophorbide a in aqueous solution may be converted into pyropheophorbide a by cleavage of the methyl ester function followed by decarboxylation. Although beyond the scope of the present study, we prepared a first-generation pyropheophorbide a–PLL conjugate and observed a similar quenching behavior as with pheophorbide a. However, these considerations have to be taken into account for the construction of second-generation PPPs and when using stock solutions of PPP.

Increased water solubility of PPP, which is highly desirable for biomedical applications, can be achieved by three different means, *i.e.* decreasing the overall MW of the polymer conjugate, introducing a hydrophilic PS instead of a hydrophobic one, and/or modifying the polymeric backbone.

Polymeric photosensitizer prodrugs made with PLL of lower molecular weight gave materials with better water solubility but less efficient quenching at equivalent PS loadings. For instance, when comparing two PPP, each of which carried 0.15 PS per lysine residue on a polymer chain, the low MW PPP made with 7.4 KDa (DP = 35.5) PLL was five-fold more fluorescent than the high MW PPP made with 25 KDa PLL (DP = 118.5). This is a very surprising finding since the maximum calculated average distance between PS in both high and low MW PPP is theoretically the same (26 Å), and the quenching should be unaffected by the chain length. Again, this fact points out that secondary structure conformation is promoting quenching and that the low MW PPP has a reduced tendency to adopt it. This is of course consistent with current foldamer theory (34) and will be the focus of our future research efforts.

In order to increase water solubility of the PPP, we switched to using the hydrophilic cationic PS PS^{3+}, depicted in Fig. 1 (23), in place of the liphophilic pheophorbide a (35). Unfortunately, this modification resulted in a PPP void of significant quenching. For instance, a PPP loaded with 30 PS^{3+} units per PLL (25 KDa) chain was only three times less fluorescent than an equimolar solution of the free PS^{3+}. The lack of sufficient quenching can be rationalized by an average increase in mutual PS distance due to repulsive interactions between these hydrophilic, positively charged PS (Fig. 1). Interestingly, fluorescent quenching by energy transfer between amphiphilic, charged, and linear near-infrared fluorophores, such as Cy5.5, has been documented by Bremer *et al.* when using similar polymeric conjugates (36), indicating important differences and requirements for quenching from chromophore to chromophore.

An alternative means to increase water solubility of our amphiphilic PS-PLL molecules was to covalently tether mPEG moieties to the polymeric backbone, which was accomplished by reacting commercially available mPEG-NHS (5 KDa) with PLL·HBr (25 KDa). This nontoxic, biocompatible polymer has been widely conjugated to many poorly soluble pharmaceuticals in order to improve on their physicochemical properties and plasma half-life (37,38). Furthermore, this experiment will help identify the most efficient protecting moieties to avoid unwanted polymeric backbone degradation of ''second-generation'' PPP. Indeed, this modification drastically improved the water solubility of the PPP, but unfortunately, it was very detrimental to the fluorescence quenching. For instance, when comparing two PPP loaded with 18 pheophorbide a units per chain and either no mPEG or 101 chains of mPEG (5 KDa), it was found that the pegylated conjugate was six times more fluorescent at equimolar concentrations of the PS (see Table 2), indicating that mPEG was interfering with the much needed PS-PS interactions and/or PPP folding. This finding is in good agreement with reports describing the deliberate use of PEG chains to reduce PS quenching in aqueous media (39). Our finding could also partly help explain the relatively modest increases in fluorescence upon enzymatic activation of chlorine e6-PLL-PEG conjugates described by Weissleder. For instance, our optimal nonpegylated PPP gave a fluorescence increase of 17.8-fold *versus* only 4.2-fold increase by the pegylated conjugate reported by Weissleder (20). Furthermore, our fully pegylated PPP gave no fluorescence increase upon trypsin digestion, indicating backbone enzymatic stability (Table 2).

Thus, we explored the use of alternative solubilizing moieties that were less likely to negatively affect quenching efficiency of the PPP and opted to only consider small, highly hydrophilic, and charged moieties such as those derived from either 1-methyl nicotinic acid or 2-(*N*,*N*,*N*-trimethylammonium) ethanoic acid. These highly hydrophilic moieties were not

Table 2. Data for PPP loaded with 18 pheophorbide a units per PLL (DP = 118.5) chain.

Solubilizer moiety	Percent solubilizer	Relative water solubility (m*M*)	Quenching factor* (F_o/FL)	Fluorescence increase† upon enzymatic degradation
None	–	1.3	137.7 ± 4.4	12 ± 0.6
2-(*N*,*N*,*N*-trimethylammonium)ethanoic acid	25	0.3	355.7 ± 14.8	12 ± 0.6
N-methyl nicotinic acid	25	> 10	426.9 ± 21.3	12 ± 0.6
N-methyl nicotinic acid	85	> 10	328.4 ± 12.6	1.2 ± 0.06
mPEG (5 KDa)	85	> 10	23.5 ± 1.0	1.1 ± 0.06

*The quenching factor was obtained as described in Table 1 at equimolar concentration with respect to the PS as determined by absorbance at 667 nm. †Maximum PPP fluorescence activation value (FL_{max}/FL, where FL is fluorescence value of the corresponding undigested PPP, and FL_{max} is maximum fluorescence value attained upon activation) upon digestion with trypsin.

expected to interact with the lipophilic pheophorbide a units. Furthermore, there are two main advantages of modifying the polymer backbone with such small entities *versus* polymeric PEG chains. First, the overall molecular weight of the conjugate does not increase drastically after introducing these moieties. Second, in second-generation PPP, the environment around the cleavage sites will be less sterically hindered and will favor enzymatic activation.

Indeed, modification of the polymer conjugate by tethering either one of these two small moieties through the respective carboxylic functions did not reduce but increased quenching efficiency of the corresponding PPP; although, surprisingly, only the moiety derived from 1-methylnicotinic acid increased water solubility of the conjugate (Table 2). The enzymatic activation of the PPP loaded with both 18 PS units per chain + 18 units of 1-methylnicotinic acid salt occurred to the same degree as the corresponding PPP carrying 18 PS units per chain and no solubilizing units. On the other hand, the PPP carrying 18 PS units per chain + 101 units of 1-methylnicotinic acid salt (100% loaded) was completely resistant to enzymatic degradation by trypsin (see Fig. 2). Thus, this small moiety can be used to modify the polymer for two purposes, namely to (1) increase water solubility of the conjugate and (ii) protect the backbone from unspecific enzymatic degradation.

In order to further elucidate the parameters dictating PPP quenching, we prepared two other conjugates made with PLL (25 KDa) carrying pheophorbide a as PS and either (1) lauric acid or (2) *p*-nitrobenzoic acid moieties covalently attached to the polymer through amide bonds between the carboxylic acid of the respective moiety and the epsilon amines of PLL. The idea was to study the effect on quenching of these moieties being able to either weaken or strengthen PS–PS interactions, respectively, through noncovalent interactions. While the PPP carrying six PS units and six lauric acid units per chain was four times more fluorescent than the reference PPP, which carried only the six PS units, the PPP carrying six PS units and six *p*-nitrobenzoic acid units was four times less fluorescent than the reference PPP. The later effect observed with the *p*-nitrobenzoic acid-derived moieties can presumably be attributed to an augmentation of PS–PS interactions by promotion of highly organized π–π-stacked structures through π–π –donor acceptor interactions (40,41). These findings reiterate the importance of PS–PS interactions required for quenching, a fact that was also illustrated by monitoring the fluorescence of undigested PPP in aqueous solutions with increasing DMSO concentrations. For a ''quenched'' PPP carrying 18 pheophorbide a units per chain, the gradual increase of DMSO concentration from 0% to 100% increased fluorescence up to 46 times. On the contrary, this solvent effect (42) was less pronounced for the ''nonquenched'' PPP carrying one pheophorbide a unit per chain, which gave a fluorescence increase of only 1.2 times under the same conditions.

Cyto-phototoxicities of our model, first-generation PPP were tested *in vitro* using the T-24 human bladder carcinoma cell line. The selectivity that would be otherwise imparted by the *in situ* enzymatic activation of the PPP was mimicked by predigestion of the PPP with trypsin. Thus, the cells were exposed to the PPP in either its active (trypsin activated) or inactive forms for 30 min, and PDT was performed with white light for 15 min (27 J cm^{-2}). The results clearly showed significant differences in phototoxicity between the two forms of the PPP as indicated in Fig. 3. Higher cell phototoxicity was observed for the activated PPP when compared with the nonactivated compound under the same irradiation conditions (see Fig. 3). As a matter of fact, the nondigested conjugate was void of any significant phototoxicity, illustrating the enormous selective potential of these PDT agents

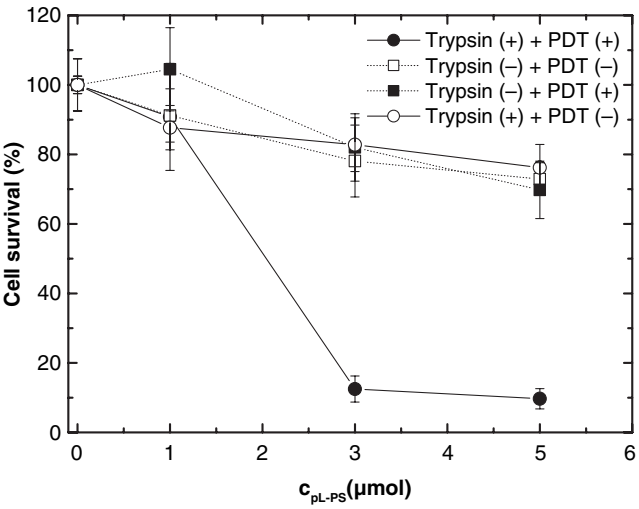

Figure 3. Cell phototoxicity of a PPP loaded with 18 PS units per chain was assessed by estimating cell viability using the MTT test. Cells were incubated with the conjugate (30 min) and subsequently washed and irradiated. The nondigested conjugate (-■-) displays no phototoxicity over the entire concentration range tested, while the trypsin-digested conjugate (-●-) is phototoxic at concentrations higher than 1 μM. No significant difference in cytotoxicity was found between the nonirradiated conjugates [nondigested (-□-) and digested-activated (-○-)] and the irradiated nondigested conjugate (-■-), indicating that the conjugates are phototoxic only in the presence of trypsin.

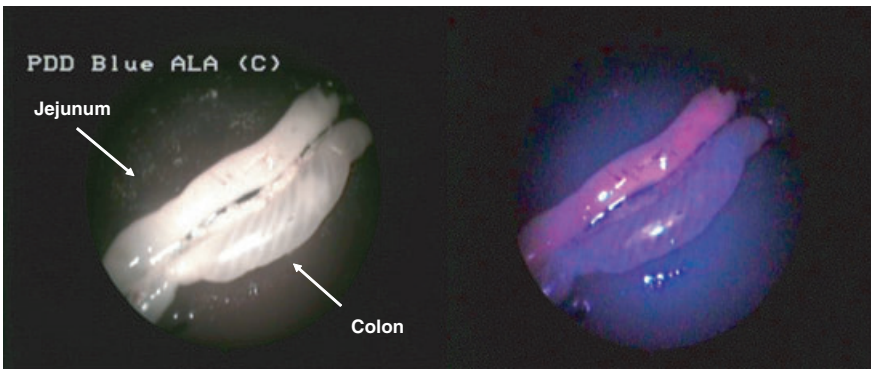

Figure 4. Mouse jejunum and colon 1 h after being instilled with a saline solution containing a PPP loaded with 18 PS units per chain (5 μM of PS) and trypsinogen (50 μg mL^{-1}) under white light (left) and blue light (right). Notice the red fluorescence originating from within the jejunum under blue light.

with minimal collateral damage. In our studies we used 30 min of incubation in order to minimize nonspecific lysosomal activation of the PPPs. However, one should take into account that the incubation time influences the PS's localization within the cells and therefore the photodynamic response (43). This will change in a real *in vivo* situation where depending on the proteolytic activity longer drug light intervals might be necessary.

In order to test the hypothesis that these PPP can be activated under physiological conditions by pathological enzymes, we performed an *ex vivo* experiment using two excised living organs, namely mouse jejunum and colon. These two organs served as models for both pathological and healthy tissues, respectively, where activation of the PPP was based on tissue ability to transform trypsinogen into active trypsin by the action of enterokinases. Thus, after having instilled the organs with an identical solution containing the PPP and trypsinogen, only the jejunum (model for pathological tissue) showed the characteristic red fluorescence (670 nm) of the activated PPP under blue light (380–400 nm) inspection (Fig. 4). Furthermore, in the absence of trypsinogen, the jejunum failed to activate the PPP.

One should take into account that depending on the interactions between the lipophilic PS units an inhibition of enzymatic cleavage might occur. However, the present data suggest that the folding shields the hydrophobic PS moieties from water but leaves hydrophilic peptide bonds exposed to solvent, where enzymes are able to access and cleave. Furthermore, even if a reduced amount of all the available peptidic linkers are exposed to the solvent, enzymatic cleavage will degrade the conjugate causing it to unfold again as all the PS are removed from the conjugate.

In conclusion, the preparation of first-generation PPP was accomplished using commercially available components, and the physicochemical properties of the resulting conjugates were easily adapted by proper choice of PS, polymer MW, and/or the use of water-solubilizing moieties. Although fluorescence quenching was more efficient than quenching of photodynamic activity, both were found to be directly correlated with PS loading. Quenching was dependent on the degree of PS loading, MW of PPP, as well as on its amphiphilicity. To illustrate this last point, PPP made with a combination of lypophilic pheophorbide a and hydrophilic PLL gave better quenching/activation behavior than a similar conjugate carrying the hydrophilic PS PS^{3+}. The quenching efficiency was attributed to reduced mean PS distance and/or orientation brought about by an unknown secondary structure, which will be the topic of future research. Modification of the PPP with mPEG or fatty acid moieties decreased quenching, while the use of *p*-nitrobenzoic acid moieties improved quenching efficiency presumably by either disrupting or enhancing PS–PS interactions, respectively. Alternatively, the PPP carrying the nitro moieties might be undergoing some other type of quenching mechanism (44). Activation of these PPP was accomplished upon backbone polymer degradation by the use of trypsin. The efficacy of these PPP to mediate PDT following enzymatic digestion was tested successfully *in vitro* and *ex vivo*.

The potential of using PPP for treating diseases such as cancer and arthritis is based on the vast body of evidence associating them with enhanced proteolytic activity, which include cathepsin B, D (12), MMP-2, MMP-7, MMP-9 (13,14) and some collagenases for cancer, and cathepsin S, K, MMP-2, MMP-9, thrombin and plasmin (45–50) for arthritis. This strategy, which has been already illustrated *in vivo* (21), has inherent advantages over conventional targeting approaches in PDT since selectivity is five-fold: (1) the use of polymer conjugates allows for passive targeting by the EPR effect, (2) proteolytic activation enables for active targeting of metabolic differences, (3) enhanced PS penetration is modulated by enzymatic digestion, (4) light is applied specifically to the desired area and (5) only oxygenated tissue will be destroyed. This last point is crucial for the PDT of diseases such as rheumatoid arthritis, where vascularized-oxygenated pathogenic tissue could be easily removed in the presence of healthy nonoxygenated cartilage.

Acknowledgements—The authors would like to thank the Novartis Foundation-Consumer Health and the Swiss National Foundation (Grant 205321-102009) for their financial support.

REFERENCES

1. von Tappeiner, H. and A. Jesionek (1903) Therapeutische Versuche mit fluorescierenden Stoffen. *Münch Med. Wochenshr.* **47**, 2042–2044.
2. Raab, O. (1900) Action of fluorescent materials on infusorial substances. *Z. Biol.* **39**, 524–546.
3. Brown, S. B., E. A. Brown and I. Walker (2004) The present and future role of photodynamic therapy in cancer treatment. *Lancet Oncol.* **5**, 497–508.

4. Moan, J. and Q. Peng (2003) An outline of the hundred-year history of PDT. *Anticancer Res.* **23**, 3591–3600.
5. Mellish, K. J. and S. B. Brown (2001) Verteporfin: A milestone in ophthalmology and photodynamic therapy. *Expert Opin. Pharmacother.* **2**, 351–361.
6. Demidova, T. N. and M. R. Hamblin (2004) Photodynamic therapy targeted to pathogens. *Int. J. Immunopathol. Pharmacol.* **17**, 245–254.
7. Jori, G. and S. B. Brown (2004) Photosensitized inactivation of microorganisms. *Photochem. Photobiol. Sci.* **3**, 403–405.
8. Maisch, T., R.-M. Szeimies, G. Jori and C. Abels (2004) Antibacterial photodynamic therapy in dermatology. *Photochem. Photobiol. Sci.* **3**, 907–917.
9. Hsi, R. A., D. I. Rosenthal and E. Glatstein (1999) Photodynamic therapy in the treatment of cancer: Current state of the art. *Drugs* **57**, 725–734.
10. Ochsner, M. (1997) Photophysical and photobiological processes in the photodynamic therapy of tumors. *J. Photochem. Photobiol. B, Biol.* **39**, 1–18.
11. Maeda, H., J. Wu, T. Sawa, Y. Matsumura and K. Hori (2000) Tumor vascular permeability and the EPR effect in macromolecular therapeutics: A review. *J. Control. Release* **65**, 271–284.
12. Fehrenbacher, N. and M. Jaeaettelae (2005) Lysosomes as targets for cancer therapy. *Cancer Res.* **65**, 2993–2995.
13. Foda, H. D. and S. Zucker (2001) Matrix metalloproteinases in cancer invasion, metastasis and angiogenesis. *Drug Discov. Today* **6**, 478–482.
14. Sternlicht, M. D. and G. Bergers (2000) Matrix metalloproteinases as emerging targets in anticancer therapy: Status and prospects. *Expert Opin. Ther. Targets* **4**, 609–633.
15. Förster, T. (1948) Intermolecular energy transference and fluorescence. *Ann. Physik.* **2**, 55–75.
16. Mahmood, U., C.-H. Tung, A. Bogdanov and R. Weissleder (1999) Near-infrared optical imaging of protease activity for tumor detection. *Radiology* **213**, 866–870.
17. Tung, C.-H., S. Bredow, U. Mahmood and R. Weissleder (1999) Preparation of cathepsin D sensitive near-infrared fluorescence probe for imaging. *Bioconjug. Chem.* **10**, 892–896.
18. Tung, C.-H., S. Bredow, U. Mahmood and R. Weissleder (2000) In vivo imaging of proteolytic enzyme activity using a novel molecular reporter. *Cancer Res.* **60**, 4953–4958.
19. Weissleder, R., C. H. Tung, U. Mahmood and A. Bogdanov (1999) In vivo imaging of tumors with protease-activated near-infrared fluorescent probes. *Nat. Biotechnol.* **17**, 375–378.
20. Choi, Y., R. Weissleder and C.-H. Tung (2006) Protease-mediated phototoxicity of a polylysine-chlorine6 conjugate. *ChemMedChem* **1**, 698–701.
21. Choi, Y., R. Weissleder and C.-H. Tung (2006) Selective antitumor effect of novel protease-mediated photodynamic agent. *Cancer Res.* **66**, 7225–7229.
22. Hackbarth, S., A. Moelich, C. Luban, S. Oelckers, F. Boehm and B. Roeder (2003) Comparative study of the photosensitization of Jukat cells in vitro by pheophorbide-a and a pheophorbide-a diaminobutane polypropylenimine dendrimer complex. *Laser Phys.* **13**, 22–29.
23. Tomé, J. P., M. G. Neves, A. C. Tomé, J. A. Cavaleiro, M. Soncin, M. Magaraggia, S. Ferro and G. Jori (2004) Synthesis and antibacterial activity of new poly-S-lysine-porphyrin conjugates. *J. Med. Chem.* **47**, 6649–6652.
24. Tedjamulia, M. L., P. C. Srivastava and F. F. Knapp (1985) Evaluation of the brain-specific delivery of radioiodinated (Iodophenyl) alkyl-substituted amines coupled to a dihydropyridine carrier. *J. Med. Chem.* **28**, 1574–1580.
25. Hora, J. (1973) Stabilization of *Bacillus subtilis* alpha-amilase by amino group acylation. *Biochim. Biophys. Acta* **310**, 264–267.
26. Mosinger, J. and Z. Micka (1997) Quantum yields of singlet oxygen of metal complexes of meso-tetrakis(sulphonatophenyl)porphine. *J. Photochem. Photobiol. A* **107**, 77–82.
27. Blagbrough, I. S., S. Carrington and A. J. Geall (1997) Polyamines and polyamine amides as potent selective receptor probes, novel therapeutic lead compounds and synthetic vectors in gene therapy. *Pharm. Sci.* **3**, 223–233.
28. Lee, M. and S. W. Kim (2005) Poly(L-lysine) and copolymers for gene delivery. In *Polymeric Gene Delivery* (Edited by M. Amiji), pp. 79–95. CRC Press LLC, Salt Lake City, UT.
29. Strand, B. L., G. Skjak-Braek and O. Gaserod (2004) *Microcapsule formulation and formation*. Focus on Biotechnology 8A (Fundamentals of Cell Immobilisation Biotechnology). 165–183.
30. Cantor, C. R. and P. R. Schimmel (1980) *The behavior of macromolecules*. W H Freeman & Co, San Francisco, CA.
31. Hackbarth, S., E. A. Ermilov and B. Röder (2005) Interaction of Pheophorbide a molecules covalently linked to DAB dendrimers. *Opt. Commun.* **248**, 295–306.
32. Doty, P. (1959) Configurations of biologically important macromolecules in solution. *Rev. Mod. Phys.* **31**, 107–117.
33. Rosenheck, K. and P. Doty (1961) The far ultraviolet absorption spectra of polypeptide and protein solutions and their dependence in conformation. *Proc. Natl. Acad. Sci. USA* **47**, 1775–1785.
34. Hill, D. J., M. J. Mio, R. B. Prince, T. S. Hughes and J. S. Moore (2001) A field guide to foldamers. *Chem. Rev.* **101**, 3893–4011.
35. Mayhew, E., L. Vaughan, A. Panus, M. Murray and B. W. Henderson (2003) Lipid-associated methylpheophorbide a (hexylether) as a photodynamic agent in tumor-bearing mice. *Photochem. Photobiol.* **58**, 845–851.
36. Bremer, C., C.-H. Tung, A. Bogdanov and R. Weissleder (2002) Imaging of differential protease expression in breast cancers for detection of aggresive tumor phenotypes. *Radiology* **222**, 814–818.
37. Scott, M. D. and K. L. Murad (1998) Cellular camouflage: Fooling the immune system with polymers. *Curr. Pharm. Des.* **4**, 423–438.
38. Zhang, G.-D., A. Harada, N. Nishiyama, D.-L. Jiang, H. Koyama, T. Aida and K. Kataoka (2003) Polyion complex micelles entrapping cationic dendrimer porphyrin: Effective photosensitizer for photodynamic therapy of cancer. *J. Control. Release* **93**, 141–150.
39. Jang, W.-D., N. Nishiyama, G.-D. Zhang, A. Harada, D.-L. Jiang, S. Kawauchi, Y. Morimoto, M. Kikuchi, H. Koyama, T. Aida and K. Kataoka (2004) Supramolecular nanocarrier of anionic dendrimer porphyrins with cationic block copolymers modified with polyethylene glycol to enhance intracellular photodynamic efficacy. *Angew. Chem. Int. Ed. Engl.* **44**, 419–423.
40. Fulton, G. P. and G. N. La Mar (1976) Proton NMR studies of the interaction of metalloporphyrins with pi acceptors and donors. I. Effect of pi-complex formation on the electronic structure of low-spin cobalt(II). *J. Am. Chem. Soc.* **98**, 2119–2124.
41. Fulton, G. P. and G. N. La Mar (1976) Proton NMR studies of the interaction of metalloporphyrins with pi acceptor and donors. II. Solution structure of the 1:1 adduct of 1,3,5-trinitrobenzene with tetra-p-tolylporphinatocobalt(II). *J. Am. Chem. Soc.* **98**, 2124–2128.
42. Savellano, M. D. and T. Hasan (2003) Targeting cells that overexpress the epidermal growth factor receptor with polyethylene glycolated BPD verteporphin photosensitizer immunoconjugates. *Photochem. Photobiol. Sci.* **77**, 431–439.
43. Kessel, D., Y. Luo, Y. Deng and C. K. Chang (1997) The role of subcellular localization in initiation of apoptosis by photodynamic therapy. *Photochem. Photobiol.* **65**, 422–426.
44. Wosnick, J. H., C. M. Mello and T. M. Swager (2005) Synthesis and application of poly(phenylene ethynylene)s for bioconjugation: A conjugated polymer-based fluorogenic probe for proteases. *J. Am. Chem. Soc.* **127**, 3400–3405.
45. Cawston, T. E. and A. D. Rowan (2005) The role of proteinases in joint tissue destruction. In *Cytokines and Joint Injury* (Edited by W. B. Van den Berg and P. Miossec), pp. 189–220. Birkhaeuser Verlag.
46. Mishiro, T., S. Nakano, S. Takahara, M. Miki, Y. Nakamura, S. Yasuoka, T. Nikawa and N. Yasui (2004) Relationship between cathepsin B and thrombin in rheumatoid arthritis. *J. Rheumatol.* **31**, 1265–1273.
47. Syrovets, T. and T. Simmet (2004) Novel aspects and new roles for the serine protease plasmin. *Cell Mol. Life Sci.* **61**, 873–885.
48. Trudel, G., H. K. Uhthoff and O. Laneuville (2005) Prothrombin gene expression in articular cartilage with a putative role in cartilage degeneration secondary to joint immobility. *J. Rheumatol.* **38**, 1547–1555.
49. Yasuda, Y., J. Kaleta and D. Bromme (2005) The role of cathepsins in osteoporosis and arthritis: Rationale for the design of new therapeutics. *Adv. Drug Deliv. Rev.* **57**, 973–993.
50. Yatabe, T. and Y. Okada (2004) MMP and ADAM in rheumatoid arthritis. *Connect. Tiss.* **36**, 223–231.